

Searching for the tetraneutron resonance on the lattice

Linqian Wu,^{1,2} Serdar Elhatisari,^{3,4} Ulf-G. Meißner,^{5,6,1,*} Shihang Shen,^{1,2,†} Li-Sheng Geng,^{2,7,1,8,9,‡} and Youngman Kim¹⁰

¹*Peng Huanwu Collaborative Center for Research and Education,
International Institute for Interdisciplinary and Frontiers, Beihang University, Beijing 100191, China*

²*School of Physics, Beihang University, Beijing 102206, China*

³*King Fahd University of Petroleum and Minerals (KFUPM), 31261 Dhahran, Saudi Arabia*

⁴*Faculty of Natural Sciences and Engineering, Gaziantep Islam Science and Technology University, Gaziantep 27010, Turkey*

⁵*Helmholtz-Institut für Strahlen- und Kernphysik and Bethe Center for Theoretical Physics, Universität Bonn, D-53115 Bonn, Germany*

⁶*Institute for Advanced Simulation (IAS-4), Forschungszentrum Jülich, D-52425 Jülich, Germany*

⁷*Sino-French Carbon Neutrality Research Center, École Centrale de Pékin/School
of General Engineering, Beihang University, Beijing 100191, China*

⁸*Beijing Key Laboratory of Advanced Nuclear Materials and Physics, Beihang University, Beijing 102206, China*

⁹*Southern Center for Nuclear-Science Theory (SCNT), Institute of Modern Physics,
Chinese Academy of Sciences, Huizhou 516000, China*

¹⁰*Center for Exotic Nuclear Studies, Institute for Basic Science, Daejeon 34126, Korea*

The nature of the tetraneutron ($4n$) system remains a pivotal question in nuclear physics. We investigate the $4n$ system using nuclear lattice effective field theory in finite volumes with a lattice size up to $L = 30$ fm, employing both a high-precision N^3LO interaction and a simplified $SU(4)$ symmetric one. The ground-state energy is found to decrease smoothly with increasing box size, showing no plateau characteristic of a resonance. We further compute the dineutron-dineutron scattering phase shift using Lüscher's finite-volume method. The phase shift is negative at low momenta, indicating repulsion in the dilute limit. At intermediate momenta, it exhibits a weak attraction with a peak of approximately 10° at relative momentum of 60–84 MeV. While this structure does not constitute a resonance, the corresponding confined $4n$ energy of 1.7–3.3 MeV lies close to the experimentally observed low-energy peak.

INTRODUCTION

Bound nuclear systems conventionally form when protons and neutrons coalesce through the strong interaction. However, the combination of attractive strong interactions and the absence of Coulomb repulsion makes the existence of pure neutron nuclei a plausible concept, a quest that dates back to the early 1960s [1]. Confirming or ruling out the existence of such neutral nuclei, whether as bound or resonant states, is crucial for advancing our understanding of nuclear physics, the strong interaction, universal fermion properties in the unitary limit [2, 3], and astrophysical objects [4, 5].

Substantial experimental and theoretical efforts have been dedicated to this challenge. In 2002, events characteristic of multineutron clusters were observed in the breakup of ^{14}Be [6]. In 2016, a candidate resonant tetraneutron ($4n$) state with an energy of $0.83 \pm 0.65(\text{stat.}) \pm 1.25(\text{sys.})$ MeV was reported in the missing-mass spectrum of the $^4\text{He}(^8\text{He}, ^8\text{Be})4n$ reaction [7]. Most notably, a recent high-statistics experiment on the $^8\text{He}(p, p^4\text{He})4n$ reaction observed a clear peak structure near the threshold at $2.37 \pm 0.38(\text{stat.}) \pm 0.44(\text{sys.})$ MeV [8].

While a bound $4n$ nucleus is generally believed to be excluded [9–11], the interpretation of these signals as a resonance remains highly debated. A variety of theoretical approaches, including Jost function analysis in the complex momentum plane [12], the hyperspherical harmonic method [13], Faddeev-Yakubovsky equations [14–16], the Gaussian expansion method [15, 16], the no-core Gamow shell model and density matrix renormalization group [17], the $4n$ response function [18], Alt, Grassberger, and Sandhas (AGS) equations [19, 20], and adiabatic hyperspherical methods [21, 22],

converge on the absence of a $4n$ resonance. The low-energy peak observed by [8] has been explained as a consequence of dineutron-dineutron correlations through a reaction model study [9]. Reactions with multi-neutron final states using a nonrelativistic conformal field theory are investigated in [23]. Recent tensor-optimized antisymmetrized molecular dynamics studies suggest that a $4n$ resonance at the nuclear surface may be influenced by core attraction [24]. For further insight into multi-neutron correlations in light nuclei, see [25].

In contrast, many-body methods that employ an external potential trap to confine the $4n$ system, subsequently extrapolating to the no-trap limit, tend to support the existence of a $4n$ resonance with energies and widths close to the experimental values. These include quantum Monte Carlo [26, 27], the no-core shell model [28], and the no-core Gamow shell model [29]. However, as discussed in Refs. [30, 31], threshold effects are critical and must be carefully accounted for in such extrapolations. For a comprehensive review of previous efforts, see [10].

To further elucidate the nature of the $4n$ signal reported in [8], additional theoretical investigations are needed. In this work, we study the $4n$ system using nuclear lattice effective field theory (NLEFT) [32, 33], a method that has proven very successful in providing a unified description of nuclear phenomena on a discretized lattice, including scattering [2, 34–36], clustering [37–40], nuclear matter [41–45], and the structure of light and heavy nuclei [46–56]. We calculate the ground-state energy of $4n$ in finite volumes up to a lattice size of $L \simeq 30$ fm. No external trap is applied, as the finite volume itself provides the necessary confinement for the dilute system.

FORMALISM

In nuclear lattice effective field theory, the many-nucleon system is solved on a discretized space with lattice spacing a and $L \times L \times L$ sites. The ground state $|\Psi\rangle$ is obtained by applying Euclidean time projection to an initial wave function $|\Psi_0\rangle$ that has nonzero overlap with the true ground state,

$$|\Psi\rangle = \lim_{\tau \rightarrow \infty} e^{-H\tau} |\Psi_0\rangle, \quad (1)$$

where the Hamiltonian H includes the kinetic energy and nucleon-nucleon interactions. We adopt the same χ EFT interaction at N^3LO order defined in Ref. [57]. The two-nucleon interaction is constrained by low-energy neutron-proton scattering phase shifts, while the three-nucleon force is fitted to the binding energies of several light and medium-mass nuclei. For further details on the interaction and the solution of the many-body system, we refer the reader to Ref. [57].

We employ periodic boundary conditions. The finite lattice box confines the nucleons, regardless of whether they form a bound state or a continuum state. To better capture the dilute nature of the $4n$ system and accelerate the convergence to the ground state in Eq. (1), we use a plane-wave Slater determinant as the initial wave function. The single-particle wavefunction is

$$\psi_{\mathbf{k}}(\mathbf{n}) = \exp\left(i\frac{2\pi}{L}\mathbf{k} \cdot \mathbf{n}\right), \quad (2)$$

with $\mathbf{n} = (n_x, n_y, n_z)$ is the lattice coordinate vector, with each component ranging from 0 to $L - 1$, and \mathbf{k} is the lattice momentum vector. The initial state $|\Psi_0\rangle$ is constructed as a Slater determinant from the two lowest momentum states, each with spin up and down. Furthermore, we perform an angular momentum projection onto the A_1^+ irreducible representation of the cubic group to project out the 0^+ state and accelerate the Euclidean time evolution [58, 59]. The ground state energy at a given projection time τ is calculated as

$$E(\tau) = \frac{\langle \Psi_0 | e^{-H\tau/2} H e^{-H\tau/2} | \Psi_0 \rangle}{\langle \Psi_0 | e^{-H\tau} | \Psi_0 \rangle}. \quad (3)$$

It is well known that the tetraneutron system lacks bound subsystems. However, when confined in a finite volume, the dineutron becomes quasi-bound. Following the method for dimer-dimer scattering on a lattice [2], we compute the $2n$ - $2n$ scattering phase shifts using Lüscher's formula. It relates the two-body energy levels in a periodic cubic box to the elastic scattering phase shifts [60, 61]:

$$p \cot \delta(p) = \frac{1}{\pi L} S(\eta), \quad \eta = \left(\frac{pL}{2\pi}\right)^2, \quad (4)$$

with $S(\eta)$ the regulated three-dimensional zeta function

$$S(\eta) = \lim_{\Lambda \rightarrow \infty} \left[\sum_{\vec{n}, |\vec{n}| \leq \Lambda} \frac{1}{\vec{n}^2 - \eta} - 4\pi\Lambda \right]. \quad (5)$$

The sum runs over all integer vectors \mathbf{n} . The energy of the two-dineutron system in the finite volume, $E^{(L)}$, is related to the relative momentum p by

$$E^{(L)} = \frac{p^2}{2\mu} - 2B_{2n} - 2\Delta B_{2n}^{(L)} \left[\sum_{\mathbf{k}} \frac{1}{(\mathbf{k}^2 - \eta)^2} \right]^{-1} \times \sum_{\mathbf{k}} \frac{\sum_{i=1}^3 \cos(2\pi\alpha k_i)}{3(\mathbf{k}^2 - \eta)^2}. \quad (6)$$

Here, μ is the reduced mass of the two dineutrons, B_{2n} is the dineutron binding energy, $\alpha = 1/2$ for the dineutron, and $\Delta B_{2n}^{(L)} = B_{2n}^{(L)} - B_{2n}$ the finite volume correction. The last term is a topological factor that accounts for the finite-volume momentum-dependent effects [62], where the summation over \mathbf{k} includes all integer vectors.

RESULTS AND DISCUSSION

We employ a lattice spacing of $a = 1.32$ fm, with L ranging from 8 to 23, corresponding to physical box sizes from approximately 10 fm to 30 fm. For comparison, we adopted an interaction with SU(4) symmetry to fit the 1S_0 scattering phase shifts. Details regarding its specific form and parameters are provided in the supplementary material.

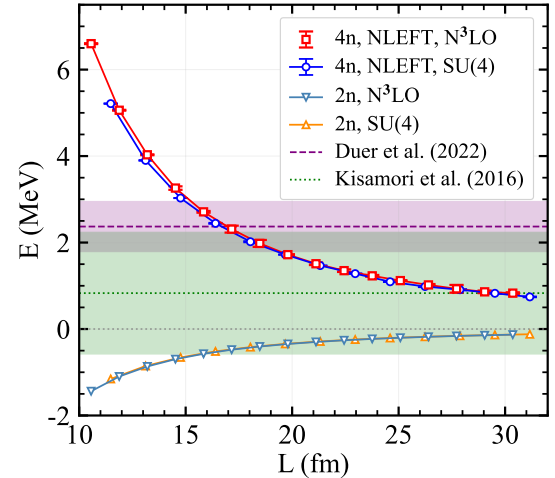


FIG. 1. Ground-state energies of the $4n$ system calculated using NLEFT with both N^3LO and SU(4) interactions, and the $2n$ system calculated using the Lanczos eigenvector method with the SU(4) interaction, as functions of the lattice size L . The error bars of NLEFT results indicate the uncertainty from the extrapolation in Eq. (S1).

Fig. 1 shows the calculated energy of the tetraneutron system at different L values, using both the full N^3LO interaction ($a = 1.32$ fm) and the simple SU(4) interaction ($a = 1.64$ fm). We also indicate candidate resonance energies from experimental studies: $E = 2.37 \pm 0.38(\text{stat.}) \pm 0.44(\text{sys.})$ MeV from Ref. [8] and $E = 0.83 \pm 0.65(\text{stat.}) \pm 1.25(\text{sys.})$ MeV from Ref. [7]. For comparison, the energy of the $2n$ system

at different L values using the SU(4) and N³LO interactions is computed via the Lanczos eigenvector method [63], which avoids Monte Carlo and extrapolation uncertainties.

Both the N³LO and SU(4) interactions yield similar results for the $4n$ system, showing strongly repulsive behavior at small L due to Pauli blocking, with energies gradually decreasing as L increases. This consistency confirms earlier findings [10, 14, 15, 17, 19, 27–29] that the tetraneutron system is insensitive to details of the nuclear interaction as long as it is realistic. The smooth, continuous decrease of the $4n$ energy lacks the characteristic plateau formation expected for resonances in finite-volume methods [64, 65], suggesting a behavior typical of a non-bound system that does not form a resonance. Furthermore, we have examined the energy derivatives and find no evidence of resonant behavior in the tetraneutron system [66].

Recent studies of the $4n$ energy distribution using the ${}^8\text{He}(p, p^4\text{He})4n$ reaction model suggest that the sharp low-energy peak observed by [8] can be explained by dineutron-dineutron correlations [9]. In a finite volume, the $2n$ subsystem becomes quasi-bound in the sense that the lowest S -wave level is shifted to negative energy relative to the two-neutron threshold, even though the infinite-volume nn system corresponds to a virtual state. This motivates us to study $2n-2n$ scattering phase shifts using Lüscher's finite-volume method, following Ref. [2]. In this context, we employ a finite-volume dineutron approximation, which means that the two-neutron subsystem is treated as an effective weakly bound dimer inside the box, characterized by a large scattering length.

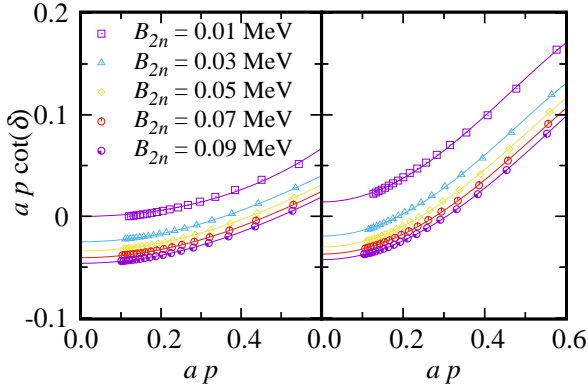


FIG. 2. Neutron-neutron ($n-n$) and neutron-dineutron ($n-2n$) scattering phase shifts calculated using Lüscher's finite-volume method with the SU(4) interaction at a lattice spacing $a = 1.64$ fm. Points represent lattice data for different B_{2n} values, and lines show fits based on the effective range expansion.

Before turning to $2n-2n$ scattering, we validate this finite-volume strategy by studying $n-n$ and $n-2n$ scattering. Since at low energies and large separations the interaction details are then suppressed, we consider the zero range leading interaction here. We tune the coupling constant of the zero-range neutron-neutron interaction so that the two-neutron subsystem is close to threshold, and we parameterize this proximity by an effective “binding” scale B_{2n} spanning 0.01 to 0.09 MeV.

We then use the resulting couplings in the two-neutron and three-neutron systems and compute the finite-volume scattering energy levels, from which we extract the phase shifts using Lüscher's method, as shown in Fig. 2. Here we define all quantities in lattice units, i.e., physical units multiplied by the corresponding power of a .

The lattice data (points) and effective-range-expansion fits (lines) show that $p \cot \delta$ versus p collapses onto the expected universal trend for all systems except at $B_{2n} = 0.01$ MeV. This behavior is related to the fact that for short-range interactions with a large two-body scattering length, low-energy observables become insensitive to microscopic details of the interaction and are governed instead by universal large-scattering-length physics associated with the unitarity (conformal) fixed point [3]. In this limit, dimensionless combinations such as $a p \cot \delta$ versus $a p$ approach universal functions, and ratios of scattering lengths (e.g., a_{n-2n}/a_{n-n}) tend toward constants, up to subleading range and regulator effects.

The behavior at $B_{2n} = 0.01$ MeV reflects that we are extremely close to the threshold regime where the intrinsic two-neutron length scale becomes very large, and small finite-volume and lattice-spacing effects can be amplified and even shift the two-body pole between a shallow bound state and a virtual state. Consistent with this interpretation, for all lattice spacings examined the neutron–neutron scattering length at $B_{2n} = 0.01$ MeV becomes large and negative, indicating a virtual state, and the neutron–dineutron system shows a similarly large and negative scattering length.

Using the effective-range expansion, we extract the ratio of neutron-dineutron to neutron-neutron scattering lengths, a_{n-2n}/a_{n-n} . The results, summarized in Table I, show a nearly constant ratio for most cases, in agreement with lattice calculations 1.176(6) [2] and semi-analytic continuum calculations 1.1791(2) [67–70]. We have verified that the results are robust against variations in lattice spacing from $a = 1.32$ to 1.97 fm [66].

Since Lüscher's relation is derived for elastic scattering, another important consistency check is that the finite-volume levels used to extract $n-2n$ phase shifts are not significantly affected by the opening of the breakup channel ($n + 2n \rightarrow n + n + n$). In the finite-volume dimer picture, the relevant inelastic scale is set by the separation energy of the quasi-bound $2n$ level, which we characterize by B_{2n} . This corresponds to a characteristic momentum scale $\sqrt{m B_{2n}}$, with m the nucleon mass. For our weakest binding this scale is small, nevertheless, even when the extracted momenta are larger than this estimate, we do not observe systematic departures from the effective-range-expansion description or anomalous volume dependence in $p \cot \delta$. This indicates that breakup (inelastic) effects are numerically negligible for the particular states and volumes analyzed here, and supports the use of the finite-volume dineutron approximation as an intermediate step toward $2n-2n$ scattering.

We now turn to the extraction of the S -wave $2n-2n$ phase shifts from our finite-volume spectra. For the realistic N³LO chiral EFT Hamiltonian of Ref. [57], the infinite-volume two-

TABLE I. Ratio of neutron-dineutron to neutron-neutron scattering lengths for different dineutron binding energies B_{2n} at a lattice spacing $a = 1.64$ fm.

B_{2n}	a_{n-2n}/a_{n-n}	error
0.01	3.35×10^{-7}	2.70
0.03	1.29	0.99
0.05	1.13	0.27
0.07	1.09	0.11
0.09	1.08	0.06

neutron system is not bound, but it corresponds to a virtual state. Nevertheless, in the periodic boxes used here the lowest nn S -wave level is shifted below the two-neutron threshold and can be treated as a shallow finite-volume dimer (a quasi-bound dineutron). This provides a practical intermediate description in which the four-neutron finite-volume levels are interpreted as two composite dimers in relative motion, and Lüscher's relation can be used to map the discrete energies to elastic $2n$ - $2n$ phase shifts.

For each box size L we compute the four-neutron energy $E_{4n}^{(L)}$ and the two-neutron energy $E_{2n}^{(L)}$ in the same periodic volume. The latter defines the effective finite-volume “binding” of the quasi-bound $2n$ level, $B_{2n}^{(L)} \equiv -E_{2n}^{(L)}$. To extract the relative momentum p of the two-dineutron system we invert the finite-volume dispersion relation for composite dineutrons, Eq. (6). This inversion requires as input the infinite-volume dineutron binding energy B_{2n} . For the N^3LO interaction this scale tends to zero as $L \rightarrow \infty$ and cannot be determined directly from our largest volumes. We therefore treat B_{2n} as an auxiliary near-threshold parameter and scan representative values $B_{2n} = 0.01\text{--}0.09$ MeV (all below the smallest $B_{2n}^{(L)}$ encountered at our largest L), using the resulting spread as an estimate of the residual systematic uncertainty associated with employing the finite-volume dineutron picture when the underlying nn pole is virtual.

The resulting $2n$ - $2n$ S -wave phase shifts are shown in Fig. 3. At the smallest extracted relative momenta (largest boxes), the phase shifts show the largest sensitivity to the auxiliary near-threshold input B_{2n} used in the inversion of Eq. (6). While some of the B_{2n} values yield slightly negative $\delta(p)$ in this regime, the low-momentum trend systematically bends toward $\delta(p) \rightarrow 0$ as $B_{2n} \rightarrow 0$, as expected for short-range interactions. We therefore do not draw a firm conclusion from the sign of the lowest-momentum points in Fig. 3. As the momentum increases, $\delta(p)$ rises, becomes positive, and exhibits a shallow maximum of order 10° around $p \simeq 60$ MeV, before decreasing again and turning negative at the highest momenta shown. The dependence on the scanned B_{2n} values is mild over most of the range and is most pronounced only at the smallest momenta, where the dineutron size is largest and finite-volume effects are maximally amplified.

In the intermediate window $p \simeq 55\text{--}100$ MeV, $\delta(p)$ displays a clear non-monotonic structure, indicating a weak at-

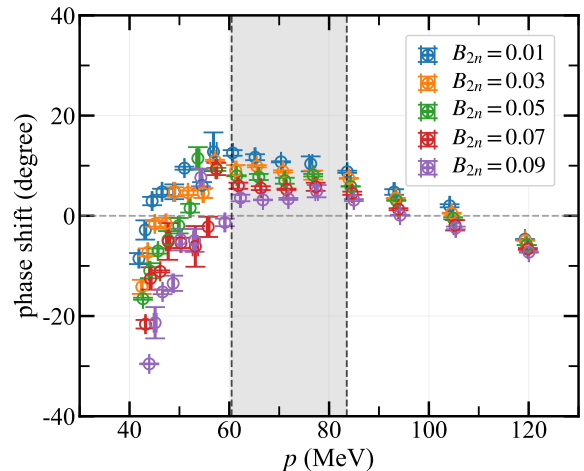


FIG. 3. Dineutron-dineutron S -wave scattering phase shift δ as a function of relative momentum p extracted from finite-volume $4n$ and $2n$ energies using Lüscher's method and the composite-dimer finite-volume relation in Eq. (6), for the N^3LO chiral EFT interaction of Ref. [57]. Different symbols correspond to the scanned near-threshold values of B_{2n} (in MeV), and the shaded band indicates the momentum range associated with $L \simeq 20\text{--}15$ fm.

tractive feature. However, we do not observe the characteristic rapid rise through 90° that would signal a narrow elastic resonance. The shaded band in Fig. 3 highlights $p \simeq 60\text{--}84$ MeV, which corresponds to $L \simeq 20\text{--}15$ fm and (for the same volumes) to confined $4n$ energies in the range $E_{4n} \simeq 1.7\text{--}3.3$ MeV (cf. Fig. 1), overlapping the experimentally reported correlated $4n$ peak at $2.37 \pm 0.38(\text{stat.}) \pm 0.44(\text{sys.})$ MeV.

SUMMARY

We have investigated the tetraneutron system confined in a cubic box using nuclear lattice effective field theory, with box sizes up to $L = 30$ fm. Using the N^3LO chiral EFT interaction, the confined $4n$ energy decreases gradually with increasing L and remains concave over the explored volumes, showing no plateau that would be characteristic of a narrow resonance. For comparison, we also repeat the confined-spectrum calculation with an SU(4)-symmetric interaction fitted to the 1S_0 phase shifts; the SU(4) results are consistent with the N^3LO trend and are reported in [66].

To interpret possible $4n$ correlations in terms of two-dineutron dynamics, we employ the finite-volume dineutron approximation, where the lowest nn S -wave level in a periodic box is quasi-bound even though the infinite-volume nn system corresponds to a virtual state. Within this framework, we validate the Lüscher-based extraction by studying n - n and n - $2n$ scattering. The ratio of scattering lengths a_{n-2n}/a_{n-n} exhibits the expected universal behavior for near-threshold systems, with deviations only when $B_{2n} \approx 0.01$ MeV, where the proximity to the virtual-state regime amplifies finite-volume and lattice-spacing effects.

We then extract the $2n$ - $2n$ S -wave phase shifts from finite-volume $4n$ and $2n$ energies using Lüscher's method together with the composite-dineutron finite-volume relation. At small momenta, the negative phase shifts indicate effective repulsion between dineutrons, consistent with effective field theory expectations near unitarity. In the intermediate window $p \simeq 55$ – 100 MeV, $\delta(p)$ becomes positive and shows a shallow non-monotonic structure, with a maximum of order 10° around $p \simeq 60$ – 84 MeV, but without a rapid rise through 90° typical of a narrow elastic resonance. This momentum band corresponds to box sizes $L \simeq 20$ – 15 fm and confined $4n$ energies of 1.7 – 3.3 MeV, which lie close to the experimentally reported correlated $4n$ peak at $2.37 \pm 0.38(\text{stat.}) \pm 0.44(\text{sys.})$ MeV.

ACKNOWLEDGMENTS

We are grateful for discussions with Kouichi Hagino, Hiroyuki Sagawa, Furong Xu, and the members of the NLEFT Collaboration. This work is supported by “the Fundamental Research Funds for the Central Universities”, National Natural Science Foundation of China under Grant No. U2541242 and 12435007. The work of SE is supported in part by the Scientific and Technological Research Council of Turkey (TUBITAK Project No. 123F464). The work of UGM was supported in by the European Research Council (ERC) under the European Union’s Horizon 2020 research and innovation programme (ERC AdG EXOTIC, Grant Agreement No. 101018170), by the CAS President’s International Fellowship Initiative (PIFI) (Grant No. 2025PD0022). The work of YK was supported in part by the Institute for Basic Science (IBS-R031-D1). LW gratefully acknowledge the Computational resources provided by the HPC platform of Beihang University, National Supercomputing Center of Korea with supercomputing resources including technical support (KSC-2024-CHA-0001, KSC-2025-CHA-0004). SS and UGM gratefully acknowledge the Gauss Centre for Supercomputing e.V. for funding this project by providing computing time on the GCS Supercomputer JUWELS at Jülich Supercomputing Centre (JSC).

* meissner@hiskp.uni-bonn.de
 † Corresponding author: sshen@buaa.edu.cn
 ‡ Corresponding author: lisheng.geng@buaa.edu.cn

[1] A. Ogloblin and Y. E. Penionzhkevich, Nuclei far from stability. treatise on heavy-ion science, edited by da bromley (1989).
 [2] S. Elhatisari, K. Katterjohn, D. Lee, U.-G. Meißner, and G. Rupak, *Phys. Lett. B* **768**, 337 (2017), arXiv:1610.09095 [nucl-th].
 [3] E. Braaten and H. W. Hammer, *Phys. Rept.* **428**, 259 (2006), arXiv:cond-mat/0410417.
 [4] T. Matsuki, S. Furusawa, and K. Suzuki, *Phys. Rev. C* **112**, 045805 (2025), arXiv:2412.19521 [nucl-th].
 [5] O. Ivanytskyi, M. Ángeles Pérez-García, and C. Albertus, *Eur. Phys. J. A* **55**, 184 (2019), arXiv:1904.11512 [nucl-th].
 [6] F. M. Marques *et al.*, *Phys. Rev. C* **65**, 044006 (2002), arXiv:nucl-ex/0111001.
 [7] K. Kisamori *et al.*, *Phys. Rev. Lett.* **116**, 052501 (2016).
 [8] M. Duer *et al.*, *Nature* **606**, 678 (2022).
 [9] R. Lazauskas, E. Hiyama, and J. Carbonell, *Phys. Rev. Lett.* **130**, 102501 (2023), arXiv:2207.07575 [nucl-th].
 [10] F. M. Marqués and J. Carbonell, *Eur. Phys. J. A* **57**, 105 (2021), arXiv:2102.10879 [nucl-ex].
 [11] C. A. Bertulani and V. Zelevinsky, *J. Phys. G* **29**, 2431 (2003), arXiv:nucl-th/0212060.
 [12] S. A. Sofianos, S. A. Rakityansky, and G. P. Vermaak, *J. Phys. G* **23**, 1619 (1997), arXiv:nucl-th/9705016.
 [13] L. Grigorenko, N. Timofeyuk, and M. V. Zhukov, *The European Physical Journal A-Hadrons and Nuclei* **19**, 187 (2004).
 [14] R. Lazauskas and J. Carbonell, *Phys. Rev. C* **72**, 034003 (2005), arXiv:nucl-th/0507022.
 [15] E. Hiyama, R. Lazauskas, J. Carbonell, and M. Kamimura, *Phys. Rev. C* **93**, 044004 (2016), arXiv:1604.04363 [nucl-th].
 [16] J. Carbonell, R. Lazauskas, E. Hiyama, and M. Kamimura, *Few Body Syst.* **58**, 67 (2017).
 [17] K. Fossez, J. Rotureau, N. Michel, and M. Płoszajczak, *Phys. Rev. Lett.* **119**, 032501 (2017), arXiv:1612.01483 [nucl-th].
 [18] R. Lazauskas, E. Hiyama, and J. Carbonell, *PTEP* **2017**, 073D03 (2017), arXiv:1705.07927 [nucl-th].
 [19] A. Deltuva, *Phys. Lett. B* **782**, 238 (2018), arXiv:1805.04349 [nucl-th].
 [20] A. Deltuva and R. Lazauskas, *Phys. Rev. C* **100**, 044002 (2019), arXiv:1910.12333 [nucl-th].
 [21] M. D. Higgins, C. H. Greene, A. Kievsky, and M. Viviani, *Phys. Rev. Lett.* **125**, 052501 (2020), arXiv:2005.04714 [nucl-th].
 [22] M. D. Higgins, C. H. Greene, A. Kievsky, and M. Viviani, *Phys. Rev. C* **103**, 024004 (2021), arXiv:2011.11687 [nucl-th].
 [23] H.-W. Hammer and D. T. Son, *Proc. Nat. Acad. Sci.* **118**, e2108716118 (2021), arXiv:2103.12610 [nucl-th].
 [24] N. Wan, T. Myo, H. Takemoto, M. Lyu, Q. Zhao, H. Horiuchi, M. Isaka, and A. Doté, *Phys. Lett. B* **864**, 139436 (2025).
 [25] S. Zhang, S. Elhatisari, and U.-G. Meißner, (2025), arXiv:2512.18849 [nucl-th].
 [26] S. C. Pieper, *Phys. Rev. Lett.* **90**, 252501 (2003), arXiv:nucl-th/0302048.
 [27] S. Gandolfi, H. W. Hammer, P. Klos, J. E. Lynn, and A. Schwenk, *Phys. Rev. Lett.* **118**, 232501 (2017), arXiv:1612.01502 [nucl-th].
 [28] A. M. Shirokov, G. Papadimitriou, A. I. Mazur, I. A. Mazur, R. Roth, and J. P. Vary, *Phys. Rev. Lett.* **117**, 182502 (2016), [Erratum: Phys.Rev.Lett. 121, 099901 (2018)], arXiv:1607.05631 [nucl-th].
 [29] J. G. Li, N. Michel, B. S. Hu, W. Zuo, and F. R. Xu, *Phys. Rev. C* **100**, 054313 (2019), arXiv:1911.06485 [nucl-th].
 [30] A. Deltuva and R. Lazauskas, *Phys. Rev. Lett.* **123**, 069201 (2019), arXiv:1904.00925 [nucl-th].
 [31] S. Ishikawa, *Phys. Rev. C* **102**, 034002 (2020), arXiv:2008.10980 [nucl-th].
 [32] D. Lee, *Ann. Rev. Nucl. Part. Sci.* **75**, 109 (2025), arXiv:2501.03303 [nucl-th].
 [33] T. A. Lähde and U.-G. Meißner, *Nuclear Lattice Effective Field Theory: An introduction*, Vol. 957 (Springer, 2019).
 [34] S. Elhatisari, F. Hildenbrand, and U.-G. Meißner, *J. Phys. G* **52**, 125102 (2025), arXiv:2507.08495 [nucl-th].
 [35] C. Wu, T. Wang, B.-N. Lu, and N. Li, *Phys. Rev. C* **112**, 014009 (2025), arXiv:2503.18017 [nucl-th].
 [36] S. Elhatisari, D. Lee, G. Rupak, E. Epelbaum, H. Krebs, T. A. Lähde, T. Luu, and U.-G. Meißner, *Nature* **528**, 111 (2015), arXiv:1506.03513 [nucl-th].

[37] E. Epelbaum, H. Krebs, D. Lee, and U.-G. Meißner, *Phys. Rev. Lett.* **106**, 192501 (2011), arXiv:1101.2547 [nucl-th].

[38] E. Epelbaum, H. Krebs, T. A. Lahde, D. Lee, and U.-G. Meißner, *Phys. Rev. Lett.* **109**, 252501 (2012), arXiv:1208.1328 [nucl-th].

[39] S. Shen, S. Elhatisari, T. A. Lähde, D. Lee, B.-N. Lu, and U.-G. Meißner, *Nature Commun.* **14**, 2777 (2023), arXiv:2202.13596 [nucl-th].

[40] S. Shen, S. Elhatisari, D. Lee, U.-G. Meißner, and Z. Ren, *Phys. Rev. Lett.* **134**, 162503 (2025), arXiv:2411.14935 [nucl-th].

[41] H. Tong, S. Elhatisari, U.-G. Meißner, and Z. Ren, (2025), arXiv:2509.26148 [nucl-th].

[42] H. Tong, S. Elhatisari, and U.-G. Meißner, *Sci. Bull.* **70**, 825 (2025), arXiv:2405.01887 [nucl-th].

[43] Y.-Z. Ma, Z. Lin, B.-N. Lu, S. Elhatisari, D. Lee, N. Li, U.-G. Meißner, A. W. Steiner, and Q. Wang, *Phys. Rev. Lett.* **132**, 232502 (2024), arXiv:2306.04500 [nucl-th].

[44] Z. Ren, S. Elhatisari, T. A. Lähde, D. Lee, and U.-G. Meißner, *Phys. Lett. B* **850**, 138463 (2024), arXiv:2305.15037 [nucl-th].

[45] B.-N. Lu, N. Li, S. Elhatisari, D. Lee, J. E. Drut, T. A. Lähde, E. Epelbaum, and U.-G. Meißner, *Phys. Rev. Lett.* **125**, 192502 (2020), arXiv:1912.05105 [nucl-th].

[46] F. Hildenbrand, S. Elhatisari, U.-G. Meißner, H. Meyer, Z. Ren, A. Herten, and M. Bode, (2025), arXiv:2509.08579 [nucl-th].

[47] Z. Ren, S. Elhatisari, and U.-G. Meißner, *Phys. Rev. Lett.* **135**, 152502 (2025), arXiv:2506.02597 [nucl-th].

[48] Y.-H. Song, M. Kim, Y. Kim, K. Cho, S. Elhatisari, D. Lee, Y.-Z. Ma, and U.-G. Meißner, (2025), arXiv:2502.18722 [nucl-th].

[49] Z.-W. Niu and B.-N. Lu, (2025), arXiv:2506.12874 [nucl-th].

[50] T. Wang, X. Feng, and B.-N. Lu, *Phys. Rev. C* **112**, 025502 (2025), arXiv:2503.23840 [nucl-th].

[51] S. Zhang, S. Elhatisari, U.-G. Meißner, and S. Shen, *Phys. Lett. B* **869**, 139839 (2025), arXiv:2411.17462 [nucl-th].

[52] F. Hildenbrand, S. Elhatisari, Z. Ren, and U.-G. Meißner, *Eur. Phys. J. A* **60**, 215 (2024), arXiv:2406.17638 [nucl-th].

[53] U.-G. Meißner, S. Shen, S. Elhatisari, and D. Lee, *Phys. Rev. Lett.* **132**, 062501 (2024), arXiv:2309.01558 [nucl-th].

[54] A. Sarkar, D. Lee, and U.-G. Meißner, *Phys. Rev. Lett.* **131**, 242503 (2023), arXiv:2306.11439 [nucl-th].

[55] B.-N. Lu, N. Li, S. Elhatisari, Y.-Z. Ma, D. Lee, and U.-G. Meißner, *Phys. Rev. Lett.* **128**, 242501 (2022), arXiv:2111.14191 [nucl-th].

[56] S. Shen, T. A. Lähde, D. Lee, and U.-G. Meißner, *Eur. Phys. J. A* **57**, 276 (2021), arXiv:2106.04834 [nucl-th].

[57] S. Elhatisari *et al.*, *Nature* **630**, 59 (2024), arXiv:2210.17488 [nucl-th].

[58] R. C. Johnson, *Phys. Lett. B* **114**, 147 (1982).

[59] B.-N. Lu, T. A. Lähde, D. Lee, and U.-G. Meißner, *Phys. Rev. D* **90**, 034507 (2014), arXiv:1403.8056 [nucl-th].

[60] M. Lüscher, *Commun. Math. Phys.* **105**, 153 (1986).

[61] M. Lüscher, *Nucl. Phys. B* **354**, 531 (1991).

[62] S. Bour, S. Koenig, D. Lee, H. W. Hammer, and U.-G. Meißner, *Phys. Rev. D* **84**, 091503 (2011), arXiv:1107.1272 [nucl-th].

[63] C. Lanczos, *J. Res. Natl. Bur. Stand. B* **45**, 255 (1950).

[64] A. U. Hazi and H. S. Taylor, *Phys. Rev. A* **1**, 1109 (1970).

[65] L. Zhang, S.-G. Zhou, J. Meng, and E.-G. Zhao, *Phys. Rev. C* **77**, 014312 (2008), arXiv:0712.3087 [nucl-th].

[66] See Supplemental Material for the energy extrapolation, the phase shifts for n - n and n - $2n$ scattering and dineutron-dineutron scattering for the SU(4) interaction.

[67] P. F. Bedaque and U. van Kolck, *Phys. Lett. B* **428**, 221 (1998), arXiv:nucl-th/9710073.

[68] P. F. Bedaque, H. W. Hammer, and U. van Kolck, *Phys. Rev. C* **58**, R641 (1998), arXiv:nucl-th/9802057.

[69] F. Gabbiani, P. F. Bedaque, and H. W. Griesshammer, *Nucl. Phys. A* **675**, 601 (2000), arXiv:nucl-th/9911034.

[70] P. F. Bedaque, G. Rupak, H. W. Griesshammer, and H.-W. Hammer, *Nucl. Phys. A* **714**, 589 (2003), arXiv:nucl-th/0207034.

SUPPLEMENTARY MATERIAL

Energy extrapolation

For each L , the energy is computed at several projection times τ and extrapolated to the infinite-time limit $E_\infty^{(L)}$ using [1]

$$E^{(L)}(\tau) = \frac{E_\infty^{(L)} + (E_\infty^{(L)} + d^{(L)}) c^{(L)} e^{-d^{(L)}\tau}}{1 + c^{(L)} e^{-d^{(L)}\tau}} \quad (\text{S1})$$

where $E_\infty^{(L)}$, $d^{(L)}$, and $c^{(L)}$ are fitting parameters. Details of the extrapolation procedure are provided in [2]. We find that the dominant contribution to the interaction energy comes from the 1S_0 channel, consistent with previous studies [3]. Other contributions, including the three-nucleon force, are negligibly smaller. For comparison, we also employ an SU(4) symmetric interaction [4] fitted to the 1S_0 phase shift, with the form:

$$V_{\text{SU}(4)} = \frac{1}{2} C_2 \sum_{\mathbf{n}} \tilde{\rho}(\mathbf{n})^2. \quad (\text{S2})$$

The density operator is defined as

$$\tilde{\rho}(\mathbf{n}) = \sum_i \tilde{a}_i^\dagger(\mathbf{n}) \tilde{a}_i(\mathbf{n}) + s_L \sum_{|\mathbf{n}' - \mathbf{n}|=1} \sum_i \tilde{a}_i^\dagger(\mathbf{n}') \tilde{a}_i(\mathbf{n}'), \quad (\text{S3})$$

where i denotes the spin index, s_L is a local smearing parameter, and $\tilde{a}_i^\dagger(\mathbf{n})$ represents the nonlocally smeared creation operator [5]:

$$\tilde{a}_i^\dagger(\mathbf{n}) = a_i^\dagger(\mathbf{n}) + s_{NL} \sum_{|\mathbf{n}' - \mathbf{n}|=1} a_i^\dagger(\mathbf{n}'). \quad (\text{S4})$$

Given the dilute nature of the system, we calculate this SU(4) interaction at a larger lattice spacing $a = 1.64$ fm for comparison. The fitted parameters are $s_{NL} = 0.1$, $s_L = 7.3918 \times 10^{-2}$, and $C_2 = -8.4272 \times 10^{-6}$ MeV $^{-2}$.

By employing Monte Carlo sampling to calculate the energies of the tetraneutron system at different values of τ for each lattice size L , and using Eq. (S1) to extrapolate to infinite projection time, the extrapolation results for both the N³LO and SU(4) interactions are obtained, as shown in Fig. S1 and Fig. S2, respectively.

Energy derivative

Following Refs. [6, 7], we compute the derivatives of the energy with respect to the box size L , as shown in Fig. S3. The numerical derivatives, particularly the second derivative for the N³LO interaction, exhibit relatively large uncertainties due to Monte Carlo sampling and projection-time extrapolation. For comparison, we also show results smoothed using the Savitzky-Golay filter [8]. In neither case do we observe the clear signature of a resonance, which would require $\partial^2 E / \partial L^2$ to cross zero. The energy curve remains concave and does not transition to convex behavior.

finite-volume extrapolation for dineutron

Figure S4 shows the finite-volume dependence of the two-neutron ground-state energy computed with the SU(4) interaction. To assess the infinite-volume limit we use an empirical exponential form, $E(L) = E_\infty + c e^{-\delta E L} / L$, and systematic large- L expansions in $1/L$. The latter follow from the threshold expansion of Lüscher's finite-volume quantization condition for short-range interactions, which predicts power-law finite-volume shifts of the lowest two-body level (with leading behavior $\propto 1/L^3$) [9–11]. Including higher order terms yields an infinite-volume energy consistent with zero, $E_\infty \approx 0$.

Phase shift

The neutron-neutron 1S_0 scattering phase shift δ , extracted from finite-volume two-neutron energies via Lüscher's method, is shown in Fig. S5. Results obtained with the SU(4) and N³LO interactions are compared with experimental data [12].

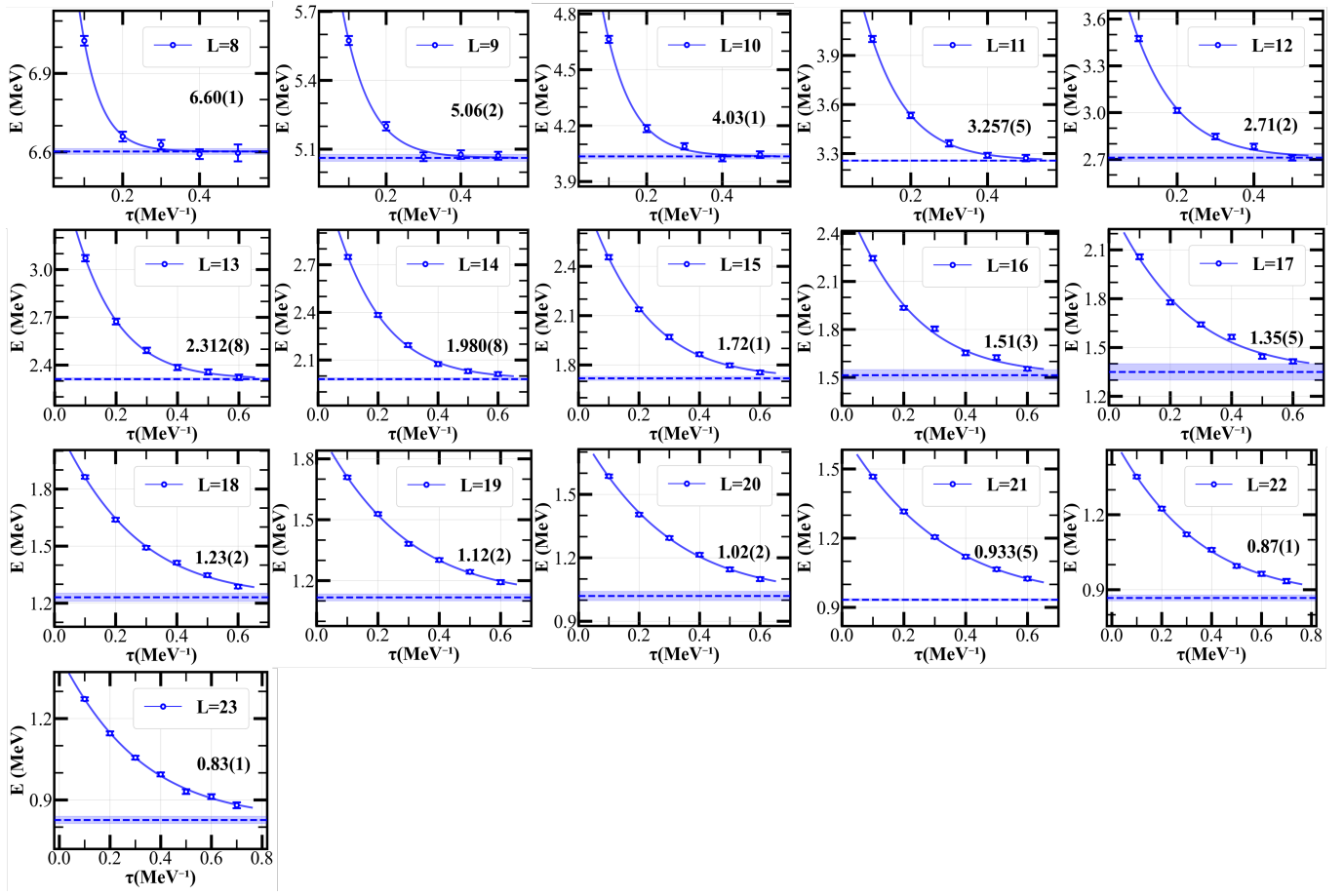


FIG. S1. The energy extrapolation of the four-neutron system with the N^3LO interaction at various lattice sizes L .

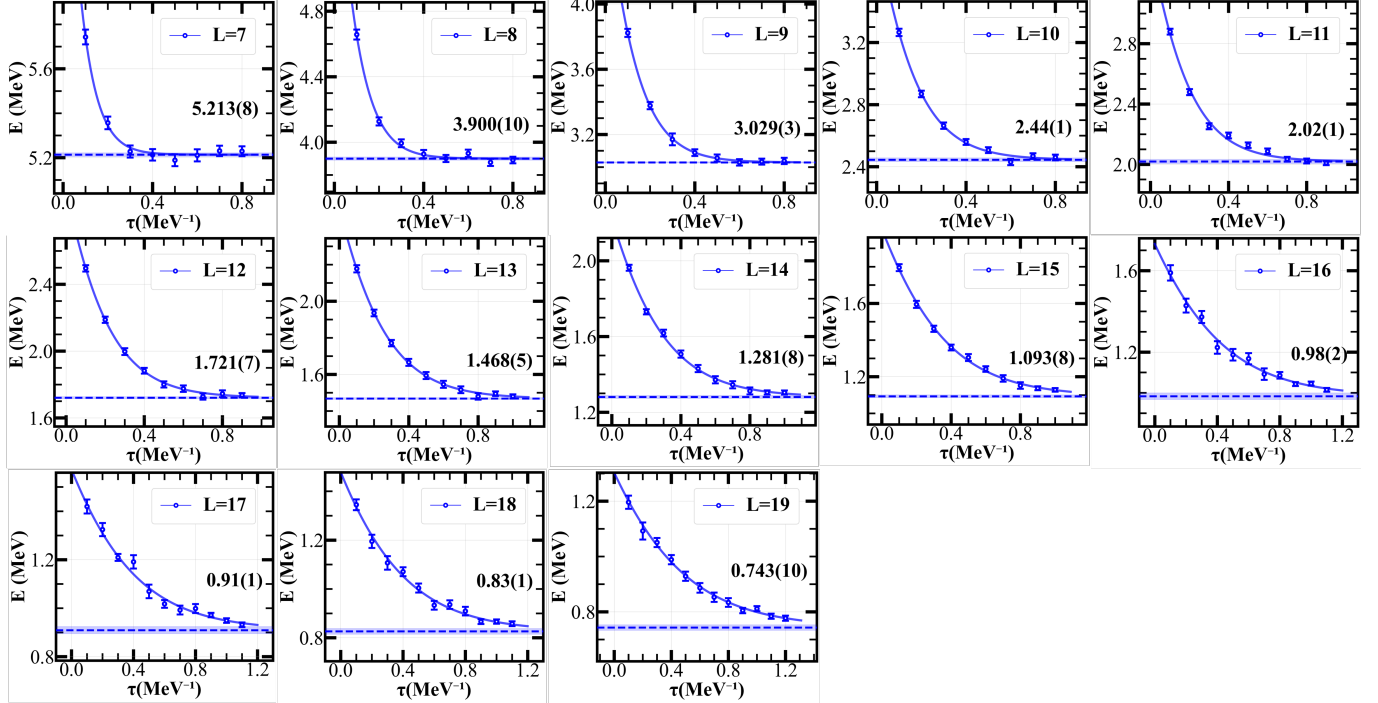


FIG. S2. The energy extrapolation of the four-neutron system with the $SU(4)$ interaction at various lattice sizes L .

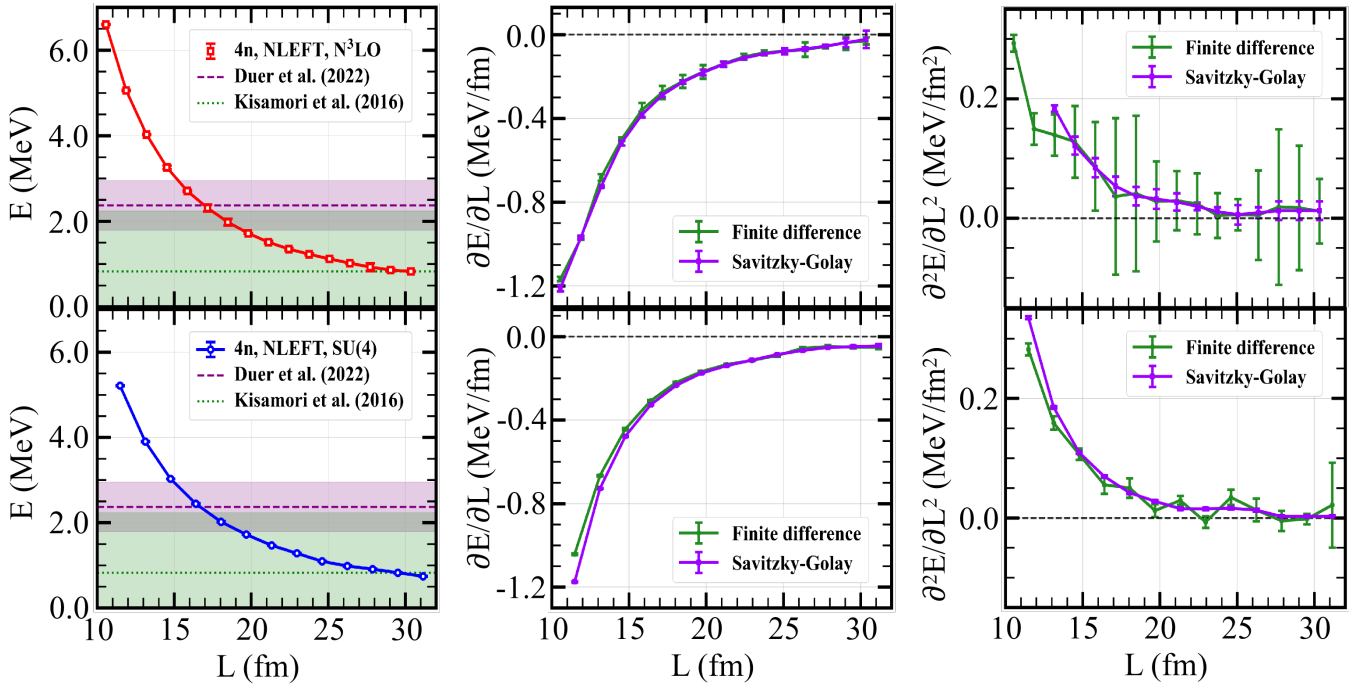


FIG. S3. Energy, energy gradient, and second derivative of the four-neutron system for the N^3LO and $SU(4)$ interactions as functions of the lattice size L .

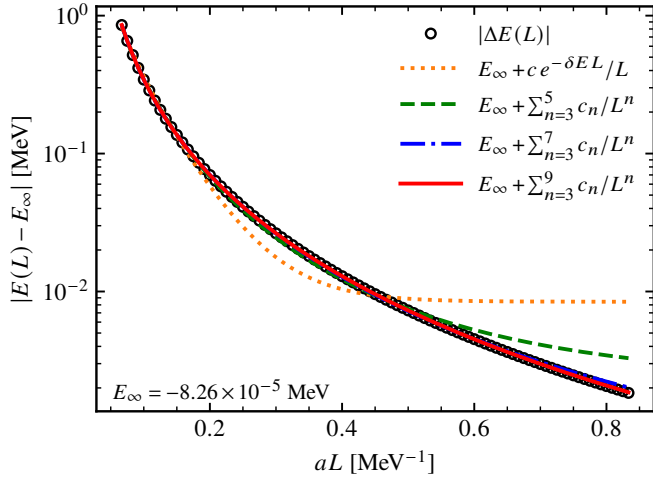


FIG. S4. Dineutron energy as a function of the cubic box length L for the $SU(4)$ interaction. The curves correspond to infinite-volume extrapolations using different numbers of terms in the fit function.

To examine whether the dineutron approximation can be used to study dineutron systems and scattering properties, we performed calculations of phase shifts for the simpler neutron-neutron and neutron-dineutron systems. The elastic two-body scattering phase shift is expanded via the effective range expansion as

$$p \cot \delta = -\frac{1}{a_{n-n}} + \frac{1}{2} r_{n-n} p^2 + \mathcal{O}(p^4), \quad (S5)$$

where p is the relative momentum of the two bodies, a_{n-n} is the neutron-neutron scattering length, and r_{n-n} is the neutron-neutron effective range. Using Eq. (S5) for extrapolation, the neutron-dineutron scattering length a_{n-2n} and effective range r_{n-2n} can also be determined by fitting the momentum and phase shift data at different L .

To test the universality of the dineutron approximation under pure contact interactions, we varied the dineutron binding energy

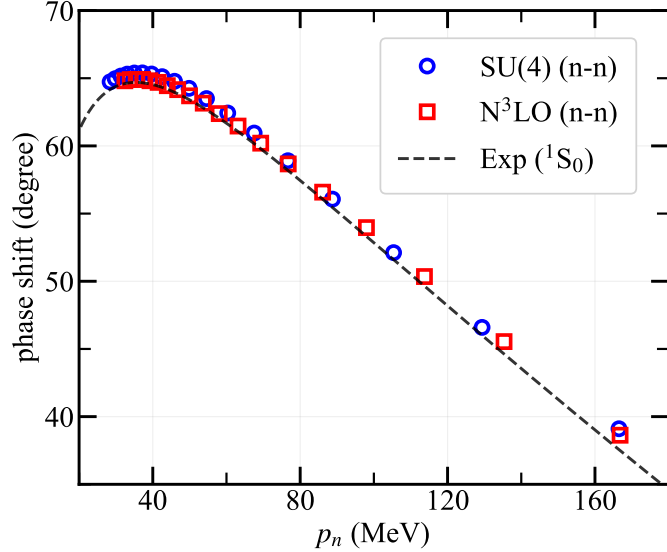


FIG. S5. Neutron-neutron 1S_0 scattering phase shift δ as a function of relative momentum p . The points are calculated from finite-volume energies using Lüscher's method for the SU(4) and N^3LO interactions, and are compared to the experimental analysis of Ref. [12].

from 0.1 MeV down to nearly zero at lattice spacings $a = 1.32, 1.64, 1.97$ fm, computed the relation between the dimensionless quantity $ap \cot \delta$ and ap as shown in Fig. S6. Except for the system with a binding energy of 0.01 MeV, all results align with the expectations, indicating the validity of the dineutron approximation.

Based on Eq. (S5), we calculated the neutron-dineutron scattering length a_{n-2n} , neutron-neutron scattering length a_{n-n} , and their ratio a_{n-2n}/a_{n-n} for different lattice spacings corresponding to a dineutron binding energy $B_{2n} = 0.01$ MeV. The results are listed in Table S1. Here, the values of a_{n-n} are large and negative across all lattice spacings, indicating a virtual state in the system, while the neutron-dineutron system also exhibits large negative scattering lengths. Additionally, Table S2 presents the ratio of neutron-dineutron to neutron-neutron scattering lengths for dineutron binding energies ranging from $B_{2n} = 0.01$ to 0.1 MeV at different lattice spacings. The results show that for lattice spacings $a = 1.32, 1.64$, and 1.97 fm, the values of a_{n-2n}/a_{n-n} exhibiting a universal behavior independent of the lattice spacing.

TABLE S1. Scattering lengths and errors for different values of a values ($B_{2n} = 0.01$ MeV).

quantity	$a = 1.32$ fm		$a = 1.64$ fm		$a = 1.97$ fm	
	value	error	value	error	value	error
a_{n-n}	-418.952822	4.714405	-3.625460×10^8	1.057483×10^{14}	-433.063197	6.848189
a_{n-2n}	-37.524722	0.948073	-67.299539	2.624853	-44.818149	0.847960
a_{n-2n}/a_{n-n}	0.089568	0.002477	1.856303×10^{-7}	0.054145	0.103491	0.002552

We also calculated dineutron-dineutron S -wave scattering phase shifts for the SU(4) interaction, as shown in Fig. S7. In the momentum range 60-120 MeV, the phase shift also shows some attraction. Similar to the case with the N^3LO interaction, no rapid rise of the phase shift to 90° is observed. The shaded region corresponds to $p \simeq 60$ -80 MeV, which for a box size of $L \simeq 20$ -15 fm yields a calculated tetraneutron energy range of $E \simeq 1.7$ -3.0 MeV.

* meissner@hiskp.uni-bonn.de

† Corresponding author: sshen@buaa.edu.cn

‡ Corresponding author: lisheng.geng@buaa.edu.cn

[1] S. Shen, S. Elhatisari, D. Lee, U.-G. Meißner, and Z. Ren, *Phys. Rev. Lett.* **134**, 162503 (2025), arXiv:2411.14935 [nucl-th].

[2] See Supplemental Material for the energy extrapolation, the phase shifts for n - n and n - $2n$ scattering and dineutron-dineutron scattering for the SU(4) interaction.

[3] R. Lazauskas and J. Carbonell, *Phys. Rev. C* **72**, 034003 (2005), arXiv:nucl-th/0507022.

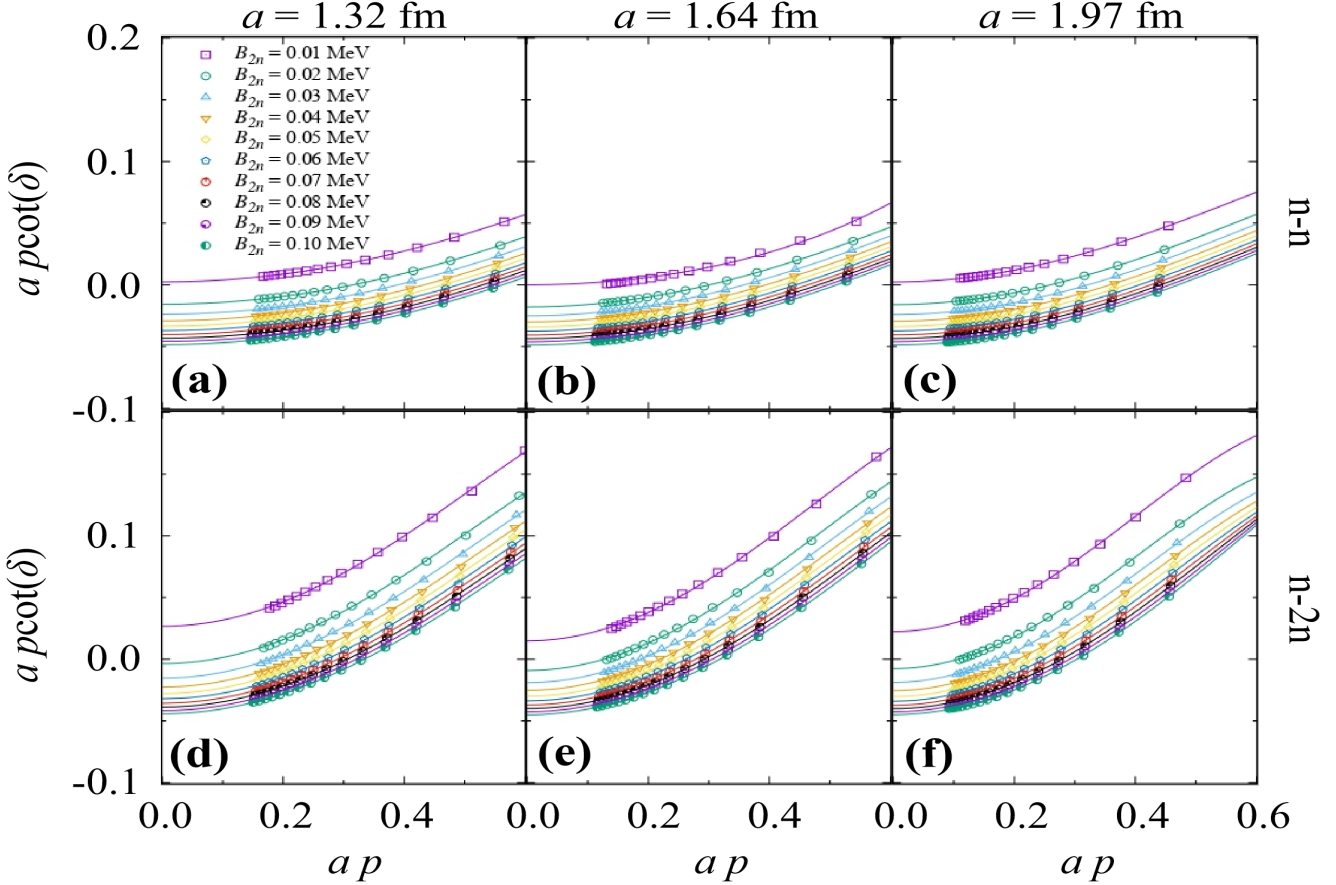


FIG. S6. Neutron-neutron (a-c) and neutron-dineutron (d-f) scattering phase shifts calculated using Lüscher's finite-volume method with the SU(4) interaction at lattice spacings $a = 1.32$ fm (a,d), 1.64 fm (b,e), and 1.97 fm (c,f). Points represent lattice data for different B_{2n} values, and lines show fits based on the effective range expansion.

TABLE S2. The ratio of neutron-dineutron to neutron-neutron scattering lengths for different lattice spacings and dineutron binding energies.

B_{2n}	$a = 1.32$ fm		$a = 1.64$ fm		$a = 1.97$ fm	
	a_{n-2n}/a_{n-n}	error	a_{n-2n}/a_{n-n}	error	a_{n-2n}/a_{n-n}	error
0.01	0.089568	0.002477	1.86×10^{-7}	0.054145	0.103491	0.002552
0.02	4.370859	0.739432	1.955848	0.104053	2.072985	0.093956
0.03	1.547733	0.054318	1.318567	0.028219	1.276168	0.018059
0.04	1.293470	0.027550	1.190182	0.015986	1.155832	0.009129
0.05	1.200866	0.018532	1.138108	0.010687	1.113122	0.005522
0.06	1.154382	0.013838	1.111648	0.007609	1.094222	0.003659
0.07	1.127364	0.010883	1.096796	0.005587	1.085393	0.002799
0.08	1.110502	0.008832	1.088154	0.004205	1.081597	0.002647
0.09	1.099464	0.007320	1.083139	0.003294	1.080561	0.002883
0.10	1.092066	0.006170	1.080411	0.002781	1.081122	0.003255

- [4] B.-N. Lu, N. Li, S. Elhatisari, D. Lee, E. Epelbaum, and U.-G. Meißner, *Phys. Lett. B* **797**, 134863 (2019), arXiv:1812.10928 [nucl-th].
- [5] S. Elhatisari *et al.*, *Phys. Rev. Lett.* **117**, 132501 (2016), arXiv:1602.04539 [nucl-th].
- [6] C. Maier, L. Cederbaum, and W. Domcke, *Journal of Physics B: Atomic and Molecular Physics* **13**, L119 (1980).
- [7] L. Zhang, S.-G. Zhou, J. Meng, and E.-G. Zhao, *Phys. Rev. C* **77**, 014312 (2008), arXiv:0712.3087 [nucl-th].
- [8] A. Savitzky and M. J. Golay, *Analytical chemistry* **36**, 1627 (1964).
- [9] M. Lüscher, *Commun. Math. Phys.* **104**, 177 (1986).

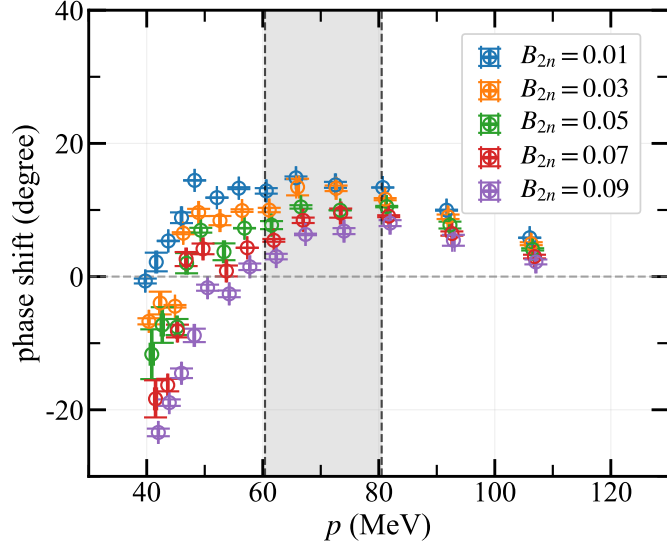


FIG. S7. Dineutron-dineutron S -wave scattering phase shift δ as a function of relative momentum p extracted from finite-volume $4n$ and $2n$ energies using Lüscher's method and the composite-dimer finite-volume relation in Eq. (6), for the SU(4) interaction. Different symbols correspond to the scanned near-threshold values of B_{2n} (in MeV), and the shaded band indicates the momentum range associated with $L \simeq 20$ –15 fm.

- [10] M. Lüscher, *Nucl. Phys. B* **354**, 531 (1991).
- [11] S. R. Beane, P. F. Bedaque, K. Orginos, and M. J. Savage, *Phys. Rev. Lett.* **97**, 012001 (2006), arXiv:hep-lat/0602010.
- [12] V. G. J. Stoks, R. A. M. Klomp, M. C. M. Rentmeester, and J. J. de Swart, *Phys. Rev. C* **48**, 792 (1993).